ARTICLE IN PRESS

Marine Geology xxx (xxxx) xxx–xxx

Contents lists available at ScienceDirect

Marine Geology

journal homepage: www.elsevier.com/locate/margo

Invited research article

Thermal subsidence and sedimentary processes in the South China Sea Basin

Ying Cao[a], Chun-Feng Li[b,c,*], Yongjian Yao[d]

[a] State Key Laboratory of Marine Geology, Tongji University, Shanghai 200092, China
[b] Institute of Marine Geology and Resources, Ocean College, Zhejiang University, Zhoushan 316021, China
[c] Laboratory for Marine Mineral Resources, Qingdao National Laboratory for Marine Science and Technology, Qingdao 266237, China
[d] Guangzhou Marine Geological Survey, Guangzhou 510075, China

ARTICLE INFO

Keywords:
South China Sea
Thermal subsidence
Sediment flux
Decompaction
Backstripping analysis
IODP Expedition 349

ABSTRACT

We coupled analysis of regional reflection seismic data with core data from International Ocean Discovery Program (IODP) Expedition 349 and found differences in both depositional features and calculated subsidence between the East and Southwest Subbasins. We calculated the original (decompacted) thicknesses of sediment for different time slices. The depositional features of the basin show that the sedimentation is controlled by both climate and tectonics. Decoupling of sedimentation rates and fluxes is often observed between the continental margin and deep basin. An abrupt increase in sedimentation rates since the Pliocene suggests that glacial–interglacial climate variability impacted erosion rates. The sedimentation rate peaked during the Pliocene in the Southwest Subbasin, but peaked during the Quaternary in the East Subbasin, showing strong influence of surrounding tectonic events, such as the buildup of Taiwan Orogen, on erosion rates. We examine thermal subsidence of the two subbasins by fitting the isostatically balanced basement depths from the seismic profiles with the half space cooling model. The estimated thermal diffusivity of the lithosphere in the Southwest Subbasin is much higher than in the East Subbasin. These contrasting observations suggest that lithospheric rock compositions may contribute to different tectonic subsidence curves between the East and the Southwest Subbasins.

1. Introduction

The South China Sea (SCS) basin is subdivided into the East, Southwest and Northwest Subbasins, and the Zhongnan Fault is considered as the boundary between the East and Southwest Subbasins (Fig. 1). The evolution of the SCS can be divided into three stages: continental rifting, seafloor spreading, and post-spreading subsidence and subduction. Rifting within the entire southeast continental margin of China occurred during the Paleogene (Shi and Li, 2012), which led to lithospheric attenuation and the formation of a series of petroliferous rift basins along the continental margin of the SCS (e.g., Lee et al., 1993; Wang et al., 2000). However, most of these basins ceased rifting after the Paleogene and are now covered by primarily non-marine sediments (Gong et al., 1997; Lee et al., 1993; Wang et al., 2000).

Ocean Drilling Program (ODP) Leg 184 in 1999 and International Ocean Discovery Program (IODP) Expedition 349 in 2014, provided better constraints on regional stratigraphy (e.g., Wang et al., 2000; Li et al., 2015a, 2015b, 2006). The improved age controls suggests that the East Subbasin of the SCS began seafloor spreading around 33 Ma and ceased spreading at about 15 Ma, whereas the Southwest Subbasin started spreading around 23.6 Ma and ceased spreading at about 16 Ma (Li et al., 2014, 2015a). This resolves many conflicting interpretations of the evolution of this region (Barckhausen et al., 2014; Briais et al., 1993; Hsu et al., 2004; Ru and Pigott, 1986; Taylor and Hayes, 1980, 1983; Yao et al., 1994).

A rapid change in the depositional environment, indicated by both sediment composition and grain size, occurred in the late Oligocene (∼25 Ma), and lasted for at least 5 m.y. (Wang et al., 2000; Li et al., 2003; Shao et al., 2004). This event was coeval to the onset of seafloor spreading in the Southwest Subbasin (Li et al., 2014, 2015b).

The closure of the SCS has been attributed to Asia-Australia collision and the rotation of the Philippine Sea Plate in the east (Hall, 2002), and the collision of continental landmasses in the Dangerous grounds and Palawan with Borneo (e.g., Hutchison, 2004). The Asia-Australia collision started at 25 Ma in Sulawesi, leading to the anticlockwise rotation of Borneo. The collision of the Luzon Arc with the Asian Plate began at about 6.5 Ma, subsequently contributing to the formation of the Taiwan Orogen and Bashi Strait (Huang et al., 1997).

Another significant post-spreading change is the sudden increase in depositional rates since ∼5 Ma along the entire northern continental

* Corresponding author at: Institute of Marine Geology and Resources, Ocean College, Zhejiang University, Zhoushan 316021, China.
E-mail address: cfli@zju.edu.cn (C.-F. Li).

http://dx.doi.org/10.1016/j.margeo.2017.07.022
Received 26 September 2016; Received in revised form 21 July 2017; Accepted 29 July 2017
0025-3227/

Please cite this article as: Cao, Y., Marine Geology (2017), http://dx.doi.org/10.1016/j.margeo.2017.07.022

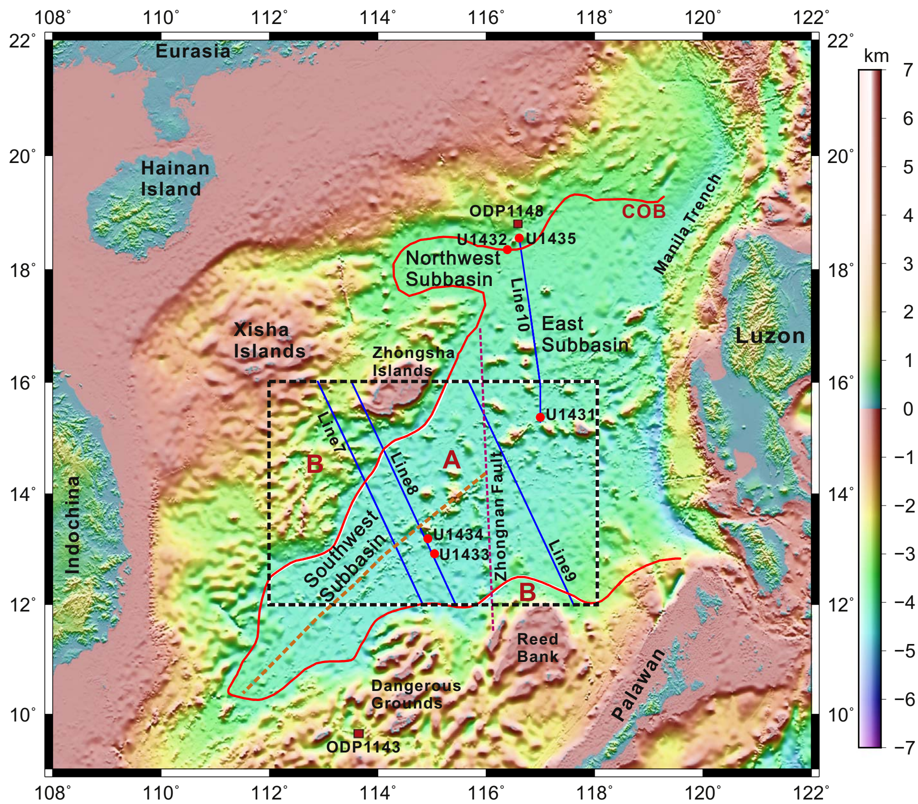

Fig. 1. Colour relief map of the South China Sea. The black square shows the area of extensive seismic interpretation in this study and the location of Fig. 3. The blue lines show the locations of seismic profile lines 7, 8, 9 and 10. The red line refers to the continent-ocean boundary (COB). The red dots and squares mark the drill sites of ODP Leg 184 and IODP Expedition 349. A and B are block subdivisions of the study area for estimating sedimentation mass and flux. Zone A in the box covers the deep sea basin, whereas Zone B covers the extended continental margin near the basin. The yellow dashed line in the Southwest Subbasin marks the relict spreading center. (For interpretation of the references to colour in this figure legend, the reader is referred to the web version of this article.)

margin and slope The dynamic mechanism is still controversial. Wang et al. (2003) attributed the accelerated deposition to the uplift of the northern margin as well as the formation of the continental shelf and large deltas. Xie et al. (2006) proposed that the dynamic topography induced by deep mantle processes can explain the accelerated post-rift subsidence at the northern margin of the SCS.

Studies of thermal subsidence and sedimentary processes in the deep basin were hampered previously for two main reasons. The first was the lack of drilling/coring constraints on stratigraphy and lack of calibration and correlation of seismic horizons. This issue has now been resolved through coring conducted during IODP Expedition 349 (Li et al., 2015a). The second problem is that no paleowater depth data are available in the central basin, making it inaccurate to use the backstripping technique for tectonic subsidence analysis.

Many differences have been observed between the East and Southwest Subbasins, including bathymetry (Yao et al., 1994), thermal state (Ru and Pigott, 1986; Li et al., 2010; Li and Song, 2012), magnetic features (Li et al., 2008), sedimentary sequences (Li et al., 2015b), and basement basalt geochemistry (Li et al., 2015a). Li et al. (2008) divided the central basin into five distinct magnetic anomaly zones and suggested that they may be attributed to different rock components of the basement or different magnetic layer thicknesses. In the central oceanic basin, the underlying basement is oceanic crust, whereas beneath the continental margins, the basement is taken as the base of the Cenozoic *syn*-rift and post-rift sedimentary sequences.

Most previous studies of sedimentary process in the SCS focused on the continental margin, where core, logging and seismic data from several research institutions and oil companies are available. Many scientists proposed that climate controlled sedimentary processes, emphasizing the impact of the summer monsoon and glacial-interglacial climate variability on sedimentation (Clift et al., 2004, 2014, 2015; Clift and Sun, 2006; Clift, 2006; Ding et al., 2016). The relative contributions of tectonics and/or climate variations to the sedimentation history of the SCS basin remain unclear and elucidating this is one of the goals of this study.

In this study, we analyze the thermal subsidence and depositional features of the SCS basin. Based on calibration to cores collected during IODP Expedition 349, we interpret 16 multichannel seismic profiles across the basin and reconstruct the original (decompacted) thickness of sedimentary layers and sedimentation rates during different geological time periods. Thermal subsidence of the two subbasins is examined by fitting the isostatically corrected basement depths from the seismic profiles with the half space cooling model, to infer their lithospheric thermal structures, rock compositions, and tectonic subsidence histories.

2. Sedimentary process in the deep basin

2.1. Decompaction analysis

Sedimentary strata need to be decompacted in order to recover their original depositional thicknesses. For this purpose, an accurate record of the porosity-depth relationship is necessary. We use the porosity data obtained during IODP Expedition 349 (Li et al., 2015a) to build a porosity-depth relationship suitable for the SCS basin. The highest porosity (80%) is observed near the seafloor, where the sediments were deposited most recently. Rather than using a single exponential fit (e.g., Royden and Keen, 1980) or linear fit (e.g., Hunt et al., 1998) for the entire depth range, we found that an exponential fit for shallow depths ($z < 150$ m below seafloor [mbsf]) coupled with a linear fit for greater depths ($z > 150$ mbsf) best captures the porosity trend (Fig. 2). The resulting equation is expressed as

$$\phi(z) = \begin{cases} 0.356\, e^{-0.00759z} + 0.426 & (z \le 150 \text{ mbsf}) \\ -2.053 \times 10^{-4} z + 0.586 & (z > 150 \text{ mbsf}) \end{cases}. \qquad (1)$$

Here $\phi(z)$ is the porosity function, and depth z is in mbsf. Fig. 2 shows all porosity measurements from IODP Sites U1431 and U1433. The data cluster closely around this curve. This consistency in the data is similar to the almost identical time-depth relationships constructed by Li et al. (2015b) for these two sites, indicating rather laterally